

Validation of Coastal Wind and Wave Fields by High Resolution Satellite Data

S. Lehner, A. L. Pleskachevsky, M. Bruck, X. Li, S. Bruschi
German Aerospace Centre (DLR), Remote Sensing Technology Institute,
Oberpfaffenhofen, 82234 Wessling, Germany

Abstract- methods to derive wind speed and the sea state from Synthetic Aperture Radar (SAR) satellite data are presented and applied for use in high resolution numerical modeling for coastal application. The new radar satellite TerraSAR-X (TS-X) images the sea surface with a high resolution up to 1m. So not only the wind field and integrated sea state parameters but also individual ocean waves with wavelengths down to 30m are detectable. Two-dimensional information of the ocean surface retrieved using TS-X data is validated for different oceanographic applications: derivation of fine resolved wind fields (XMOD algorithm) and integrated sea state parameters (XWAVE algorithm). The algorithms are capable to take into account fine-scale effects in coastal areas.

The wind and sea state information retrieved from SAR data are applied as an input for a wave numerical spectral model (wind forcing and boundary condition of sea state) running at fine spatial horizontal resolution of 100m. The results are compared to collocated buoy measurements. The sea state simulated by increased and decreased wind speed and comparison against waves simulated using original TS-X derived wind shows sensitivity of waves on local wind variation and thus the importance of local wind effects on wave behavior in coastal areas. Examples for the German Bight, North Sea are shown.

The TS-X satellite scenes render well developed ocean wave patterns of well developed swell at the sea surface. Refraction of individual long swell waves at a water depth shallower than about 70m is caused by the influence of underwater topography in coastal areas which is imaged on the radar scenes. A technique was developed for tracking of wave rays depending on changing of swell wavelength and direction. We estimate the wave energy flux along the wave tracks from deep water to the coastal line based on SAR information: wave height and wavelength are derived from TS-X data.

I. INTRODUCTION

Since 2007 a number of new high resolution X-band radar satellites have been launched, that yields the

possibility to image and measure the wind field and the sea state at high resolution. This is particularly useful when investigating coastal wind and wave fields.

The estimation of marine and meteorological parameters is an important task for operational oceanographic services. Numerous techniques of *in-situ* measurements, global, regional and fine-resolution forecast models are used to give information on wind parameters, sea state and connected processes. The global coverage and independency from input data gives a special position for space borne instruments and satellite based techniques in comparison to *in-situ* methods and mathematical simulations. Remote sensing data, in particular from space borne SAR, are an irreplaceable source for model validation and verification in the open sea and coastal zones due to their independence from sunlight illumination and cloud coverage.

The forecast modeling services, e.g. by the German Weather Service (DWD, www.dwd.de) are a part of global marine weather and warning system. Wave forecasting in the trans-ocean shipping routes, storm prediction, wave and wind related information for coastal protection and sport boats are important. Nowadays wave models of the III generation have been developed and are used for sea state prediction, e.g. global WAVEWATCH III by NOAA (<http://polar.ncep.noaa.gov/waves/viewer.shtml>). In the open sea the wave models are already capable to produce a considerable and high-quality forecasting service [1], as long as the wind input from atmospheric forecast models and boundary conditions for sea state are correct.

On the global scale the difficulties arise when forecasting rapid development of strong storms with gustiness, which are occasionally "not captured" by atmospheric model predictions and thus do not correctly reproduce ocean waves ([6], [18]). During heavy storms in the North Sea like "Anatol" on Dec. 03, 1999 and "Britta" on Nov. 01, 2006 the forecast atmospheric models, the input for the wave simulation, were not capable to predict such a rapid progressive increase of wind. Correspondingly, both of the storms were underestimated in respect to wave forecast and results in accidents and destruction on the shore construction. An example is the damage on the offshore research platform FINO-1, where the metal constructions in 18m over mean sea level were destroyed by waves. These

incidences have shown the vulnerability of offshore industry significantly constructions in storm weather conditions.

Furthermore uncertainties are investigated when dealing with numerical modeling in coastal areas where physical processes in shallow water, caused by interaction between waves, currents and bottom become important. The wave properties are changing strongly in spatial domain in coastal areas. The ocean waves propagation towards the shore present conversation of energy flux, influenced by energy dissipation due to bottom friction and wave breaking. The variable depth in shallow areas results in depth-forced changing of wave length and wave height. The shortening of the wavelengths is compensated by wave height increase (shoaling effect). Due to bottom influence the wave energy is dissipated and transferred into turbulence and acceleration of flow currents (radiation stress). As a result, the current structure will undergo a significant change at the coast and around the sandbanks, where dissipation is strongest. In the German Bight a long-shore current of some $30\text{-}50\text{cm}\cdot\text{s}^{-1}$ magnitude appears in near-shore zone approximately 0.5km wide. Local variations can exceed $2\text{m}\cdot\text{s}^{-1}$ if waves are completely dissipated due to large localized topographic gradients under storm conditions [10].

Thus, significant efforts are needed accordingly to implement shallow water interaction into numerical schemes by coupling of wave and circulation models through radiation-stress and by tuning of the model functions and parameters. Such forecasts coupled model systems have been developed by different organizations (DELTA RES, DWD, HZG) and need data for validation. For this purpose SAR data from high resolution TerraSAR-X images can be successfully applied.

In this paper, new methods to retrieve wind [12] and sea state [2],[4] information are used in order to show the possibility of using SAR-derived data for coastal numerical model validation. Since the methods are based on using data with high resolution they allow to obtain the parameters with respect to fine-scale effects in coastal areas. The wind and sea state parameters obtained from SAR were implemented into a numerical spectral wave model, run on high spatial resolution of 100m . This way the validation of models can be performed at a new qualitative stage.

The paper is structured as follows: in section 2 the data are briefly introduced and the methods to retrieve wind, sea state and underwater topography are discussed. Section 3 deals with implementation of the derived information into numerical modeling.

II. TERRASAR-X SATELLITE, DATA AND ALGORITHMS

In this section the characteristics of the new German radar satellite TerraSAR-X are described. The examples of SAR images from different modes are used to obtain wind and sea state.

A. TerraSAR-X satellite

The space borne SAR (Synthetic Aperture Radar) as a remote sensing instrument is a unique sensor to provide two dimensional information of the ocean surface. Due to their high resolution, daylight and weather independency and global coverage, space borne SAR's of new generation are particular suitable for many ocean and coastal applications [13]. In the paper presented here data from the radar satellite TerraSAR-X (TS-X) are used [3] to provide meteorological and marine parameters.

The X-band SAR satellite TS-X was launched in June 2007 (www.dlr.de/TerraSAR-X). Since January 2008, data and products are available for researchers and commercial customers. TS-X operates from 514km height at sun-synchronous orbit, the TS-X ground speed is $7\text{km}\cdot\text{s}^{-1}$ (15orbits per day). It operates with a wavelength 31mm and frequency 9.6GHz . The repeat-cycle is 11 days, but the same region can be imaged with different incidence angles after three days dependent on scene latitude. Typical TS-X incidence angles range between 20° and 55° .

B. TerraSAR-X imaging modes

TS-X operates four different basic imaging modes with different spatial resolution, technical parameters of the modes are provided in Fig.1. The analysis of TS-X images is used for the different applications: ship-, ice-, oil- and underwater shallow area (bank and bars) detection as well as measuring the wind fields [12], coastal line and underwater topography fields. In this paper we investigate sea surface observed on TS-X Spotlight images with coverage of 10km by 10km and Stripmap images with coverage of 30km by 50km to 100km .

Examples of TS-X images acquired over the North Sea (Stripmap and high-resolution Spotlight) are shown in Fig.2. The Stripmap scene imaged over the Elbe-Estuary on Nov. 11, 2008 (low tide) depicts the changing of bathymetry in the estuary in comparison to bathymetry processed by BAW (German Federal Waterways Engineering and Research Institute) in 2006. As the TS-X image shows, a long sandbank was partially eroded in the centre and split by a tidal inlet.

Compared to other SAR missions like ENVISAT ASAR TS-X offers besides higher resolution a number of further advantages: e.g. Doppler-shift of scatterers, moving with radial velocity u_r toward the sensor at distance R_o (slant range) are reduced. For instance, for the same incidence angle 22° and $u_r=1\text{m}\cdot\text{s}^{-1}$ the target's displacement in azimuth $D_x = (u_r / V_{sar}) \cdot R_o$ [15] is reduced by factor about two and results in $\sim 73\text{m}$ for TS-X and $\sim 115\text{m}$ for ENVISAT due to different platform velocity V_{sar} ($7,55\text{km}\cdot\text{s}^{-1}$ for ENVISAT) and slant range R_o (ENVISAT altitude is 800km) yields better possibilities to measure sea state, in particular a cut-off of minimal imaged wavelength is reduced up to 30m . Fig.4 shows statistics over distribution the observed peak

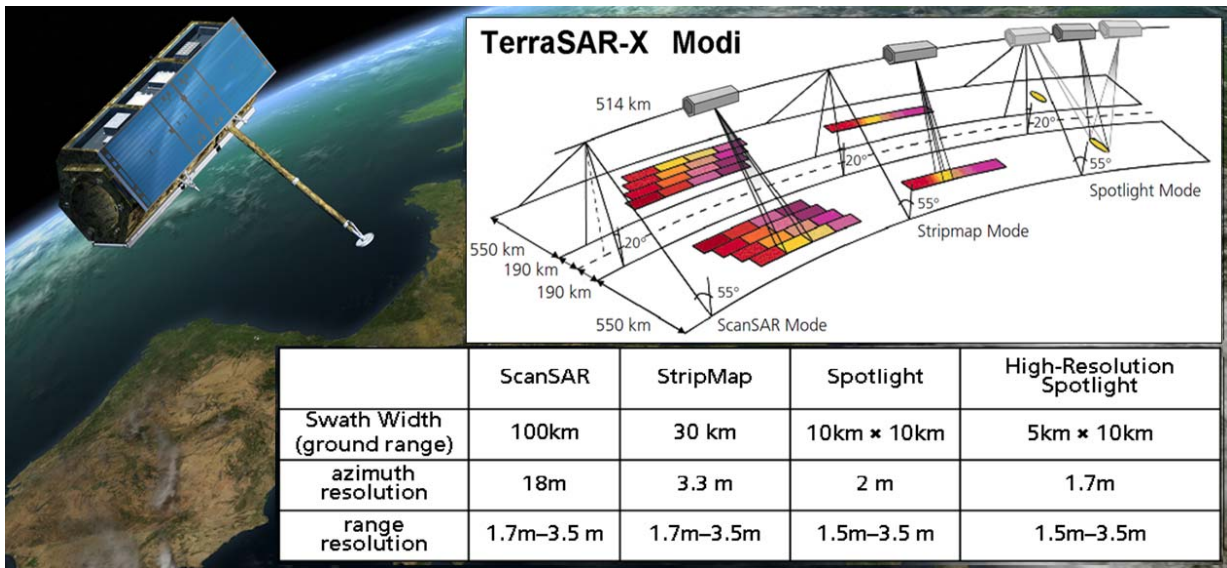


Figure 1. TerraSAR-X satellite and characteristics of four TS-X modes: ScanSAR, Stripmap, Spotlight and High-Resolution Spotlight.

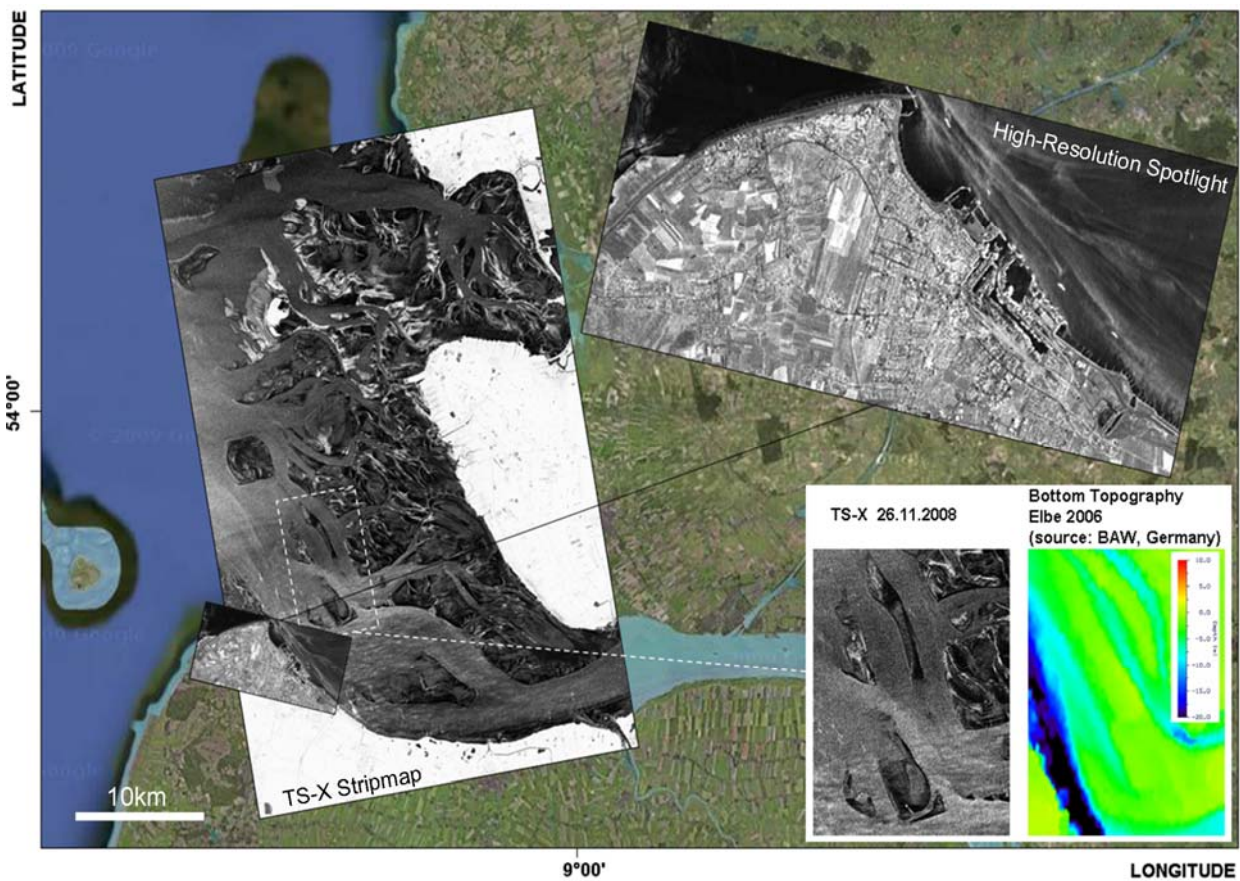


Figure 2. TerraSAR-X scenes acquired over Elbe Estuary, German Bight, North Sea (background image © Google Maps): Stripmap scene acquired on November 26, 2008, 17:10 UTC (low tide) and Spotlight scene on December 12, 2007 05:50 UTC. The Stripmap scene depicts the change of bathymetry of Elbe Estuary since 2006, when the BAW bathymetry map was completed (sub-scene below right: a long vertical bank was partially eroded and split by an inlet).

wavelength for different wave traveling direction for 100 TS-X scenes acquired in the North Sea, (cut-off is colored gray). For the azimuth traveling waves the minimal wavelength observed is 100m, for the range traveling wave the value of the minimal observed wavelength is about 30m.

C. XMOD algorithm to obtain wind fields.

Synthetic aperture radar is capable of providing wind information over the ocean by measuring the roughness of the sea surface. The SAR wind field retrieval approach was first developed for C-band SAR data that are for example provided by ERS-2 and ENVISAT ASAR, e.g., CMOD4 or CMOD5 [12]. An X-Band Geophysical Model Function (GMF) algorithm (XMOD) was established for VV and HH polarized data to obtain the wind fields [17]. The relationship between X-band radar cross section and wind speed, wind direction and incidence angle is applied; wind field parameters can be retrieved accurately for incidence angles θ of $20^\circ\sim 60^\circ$ and wind speed in the range $2\text{m}\cdot\text{s}^{-1}\sim 20\text{m}\cdot\text{s}^{-1}$. The existing C-band techniques (CMOD) have been extended by developing X-band geophysical model function XMOD given by:

$$\sigma_o(U, \theta, \varphi) = x_o + x_1 U + x_2 \sin(\theta) + x_3 \cos(2\varphi) + x_4 U \cos(2\varphi) \quad (1)$$

where σ_o is NRCS, U is the wind speed, φ is the wind direction. The constants x_i $i=0,4$ are tuned using the measurement data sets. To determine wind direction, streak structures on the sea surface of the image are used. These are supposed to be produced by airflow turbulent eddies at boundary layer. Shadows behind the coast give evidence of wind blowing from the coast.

Data from the Spaceborne Imaging Radar-C/X (SIR-C/X) mission in 1994 and from the European Center (ECMWF) reanalyzed wind fields ERA-40 (ECMWF Re-Analysis of the global atmosphere and surface conditions for 45-years) were used to tune the algorithm; the comparisons are given in [16]. The results are validated using *in-situ* measurements from collocated buoys and modeled data with different resolution, (HIRLAM model and DWD COSMO). Fig.3 shows the wind field derived from a TS-X Stripmap scene acquired on March 26, 2008 at 05:41 UTC over Sylt Island located in the North Sea.

The retrieved wind field shows fine-scale turbulence effects, shadowing of the island is visible in the TS-X obtained wind: the wind speed is slow down from about $13\text{m}\cdot\text{s}^{-1}$ to $10\text{m}\cdot\text{s}^{-1}$. The use of wind data obtained from TS-X SAR images into numerical modeling and comparison of simulated wave height against collocated buoy measurements show a good agreement with derived wind speed and direction (more details see section 3). The wind field can be retrieved practically to 20m resolution by the XMOD algorithm for TS-X images. This influences model results of the sea state, which is strongly dependent on local wind.

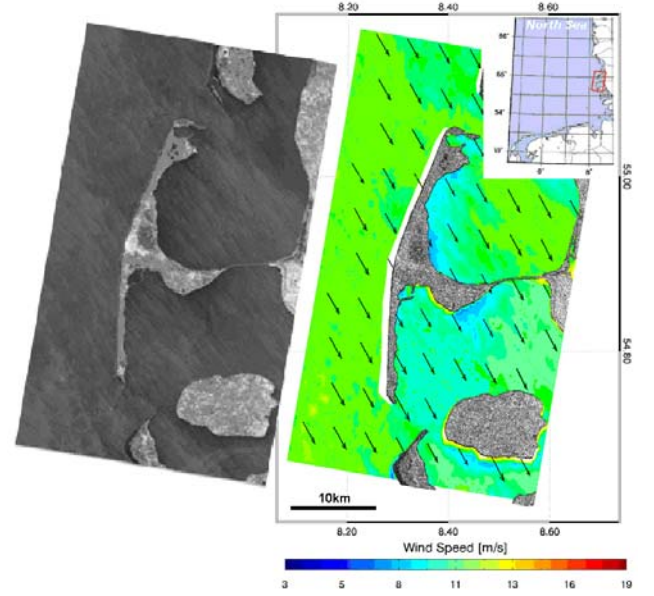


Figure 3. Wind speed retrieved from HH polarized Stripmap data of TerraSAR-X acquired over Sylt Island, North Sea on March 26, 2008 (left, wind speed errors due to insufficient information are masked (white color), top right the location and quicklook are show).

The XMOD linear algorithm yields reasonable measurement for wind up to about 15m/s. A new algorithm XMOD-2 has been developed that takes the full nonlinear physical model function into account [14].

D. XWAVE algorithm to derive integrated wave parameters

An empirical X-WAVE model for obtaining integrated wave parameters (wave height and period) has been developed for X-band data [13]. The algorithm is based on analysis of image spectra and uses parameters fitted with collocated buoy data and information about spectra peak direction and incidence angle. The algorithm to derive significant wave height from TS-X SAR data presented by the equation:

$$H_s = x_1 \cdot \sqrt{E(1.0 + \cos(\alpha))} + x_2 \quad (2)$$

where α is the wave peak direction related to the azimuth direction ($0^\circ \leq \alpha \leq 90^\circ$). The cosine function in the formula describes the dependence of wave peak direction in the image relative to satellite direction, E is the integrated value of the directional wave number spectrum. The coefficients x_i dependent on incidence angle θ are determined from a linear fitting between E and the collocated significant wave height, computed by the DWD wave model. Peak period T_p corresponds to the wave period for which the energy is maximum in the 2D spectrum in frequency domain.

For the validation and tuning of the XWAVE algorithm, different data sets were used: collocated buoy measurements, WaMoS II (Wave Monitoring System, [2]) radar data and DWD wave hindcast model results ([7], [17]). Comparison of TS-X derived significant wave height with the significant wave height obtained by the buoy located at the Ekofisk oil

platform in North Sea (56°10'03"N 3°32'32"E) shows a correlation of 0.83. TS-X derived peak wave length for NDBC buoy 44066 (39°34'59"N 72°36'2"W) and from the buoy located near Ekofisk oil platform have a correlation of 0.95, a scatter index of 0.19, mean square error of 0.89 (53 entries) and thus show a good agreement with in-situ data (Fig.4). More details are given in [4].

E. Wave ray tracing

In coastal areas the refraction of long swell waves at water depth shallower than 70-50m is caused by the influence of the underwater topography. Ocean surface waves begin to change its properties if the water depths become lower than about half of the wavelength. If a long ocean swell is propagating into shallows, the wavelength begins to shorten and the wave height increases due to conservation of energy.

The tracking of wave rays is based on following a wave in its propagation direction from a start point up to the coast. The wave-rays technique is already well known and used as an application for wave model results (e.g. [22]). The wave rays can be obtained also from wavelength and wave direction observed on SAR images [7].

The algorithm to obtain wavelength and direction from TS-X SAR images is given in [7]. Around a selected point on the image (starting point of the wave track) a sub-image is selected. By computing the Fast Fourier Transformation (FFT) for the selected sub-image a two dimensional image spectrum in wave number space is retrieved. The peak in the 2D spectrum marks mean wavelength and mean wave direction of all waves visible in the sub-image. Values for wavelength and angle of propagation can be obtained by the following formulas:

$$L_p = \frac{2\pi}{\sqrt{k_x^2 + k_y^2}}, \theta_p = \arctan\left(\frac{k_{p,y}}{k_{p,x}}\right) \quad (3)$$

where L_p is the peak wavelength and θ_p is the peak wave direction with respect to the image, $k_{p,x}$ and $k_{p,y}$ are the peak coordinates in wave number space. The retrieved wave directions have an ambiguity of 180° due to the static nature of a SAR image.

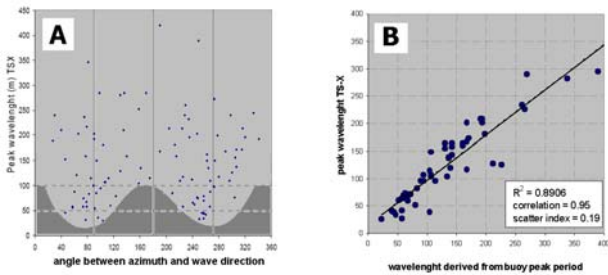


Figure 4. distribution of peak wavelength over direction from 100 TS-X scenes acquired in North Sea – the cut-off is grey colored (wavelength about 30m for range and about 100m for azimuth directions) (A). Scatter-plot for peak wavelength derived for collocated buoys (NDBC 44066 28 entries and by Ecosfisk Platform 27 entries) and TS-X (B).

This ambiguity can be resolved using the SAR cross spectra or first guess information from other sources or from complex SAR data. In coastal areas where wave shoaling and refraction appears the propagating direction towards the coast is visible on the image [11].

Starting in the open sea the box for the FFT is moved in wave direction by one wavelength and a new FFT is computed. This procedure is repeated until the corner points of the FFT-Box reach the shoreline. This way, a wave can be tracked from the open sea to the shoreline and changes of wavelength and direction can be measured. Wind streaks and wind sea patterns are removed from the spectra by filtering for analyzed wavelengths between 80 and 300 meters (background values must be checked for every scene). After moving the FFT-box to the next point in swell propagation direction the next peak is restricted to deviate no more than +/-15° compared to previous peak direction in order to avoid switching to another wave system in the case of a cross sea.

F. Underwater shallows and determination of energy flux

The TS-X scene acquired in the North Sea on Feb. 25, 2009 over Helgoland Island depicts swell waves about 0.3-0.7m wave height and length about 100-160m propagating direction SE in German Bight. The simulated wave rays (Fig.5) show a connection with underlying depths and shallows. The information derived from this scene is insufficient to retrieve the precise depth map using dispersion relation due to weak swell wave height for whole SAR scene, but more than sufficient to detect underwater bars and sandbanks (swell waves with about $H_s > 0.5m$ will allow to obtain underwater topography, [7]). This kind of information is important for areas such as the German Bight, where the soft seabed can be changed relatively fast due to storms, so the official charts can be out of data.

Data of wave impact on the coast and beaches are important for aftermath risk estimations used for the planning of engineer measures and coastal management or oil platforms. To obtain this information is a complicated task for coastal protection. One method is getting the information from wave rider buoys by *in-situ* measurements: the measured wave parameters are used to estimate the wave energy on the buoy location. Using mathematical formulas the energy flux and energy dissipation on the coast are extrapolated [21]. Using wave models this process can be calculated without extrapolations [10].

New possibilities to obtain the energy flux give high resolution TS-X SAR data: the wave parameters can be estimated and the energy flux can be determined along a wave ray. The energy flux (power transported by waves [$J \cdot m^{-1} \cdot s^{-1}$]) is given by:

$$F = E_w c_g \quad (4)$$

where E_w is the mean wave energy density per unit horizontal area ($J \cdot m^{-2}$) and c_g is the wave group velocity. E_w we estimate from significant wave height H_s , obtained from TS-X image using XWAVE algorithm. The group velocity

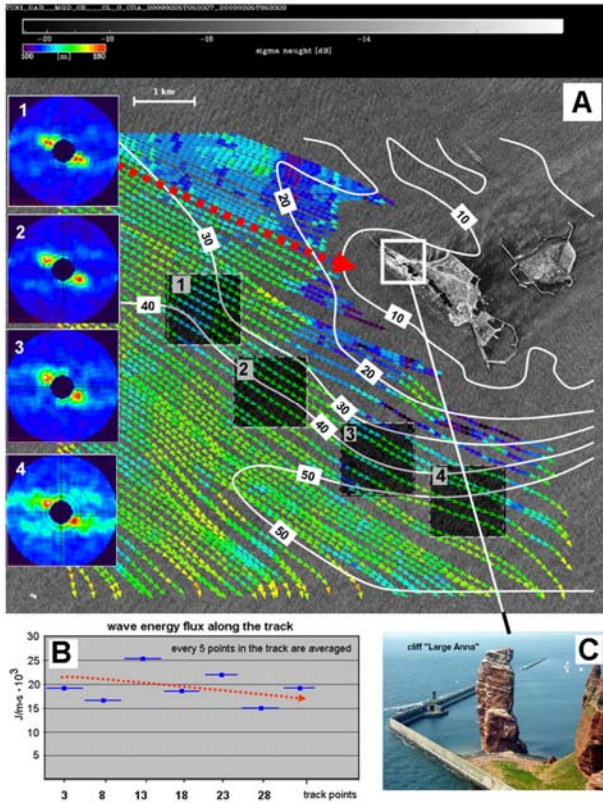


Figure 5. TS-X Spotlight acquired in the North Sea on February 25, 2009 over Helgoland Island Helgoland area: wave ray tracking depicts the shallow areas (isolines for depths of 10,20,30,40,50m are shown) (A). The normalized image spectra are shown for four sub-scenes. Color bar means the value of wavelength. Energy flux for one wave ray (red line) (B). Cliff "Large Anna" (C).

is estimated from phase speed c_p of swell peak wavelength from the corresponding location of tracked wave ray. An example is shown in Fig.5 (one track to shore where cliff "Large Anna" is located).

The cliff "Large Anna" is a protected nature phenomena demolished by waves. For its protection a concrete construction was installed (see photo sub-image down). To obtain the wave energy flux along the wave track the information was averaged for every 5 points along the track. The mean value of about $20\text{kJ}\cdot\text{m}^{-1}\cdot\text{s}^{-1}=20\text{kW}\cdot\text{m}^{-1}$ (swell) was calculated using SAR information. The spread in the graph results from differences of obtained H_s : the mean value of swell wave height is about 0.8m and varies by about $\pm 0.2-0.4\text{m}$.

G. Underwater topography estimation

As in shallow areas, bathymetry is reflected by long swell wave refraction governed by underwater seabed structures, the depths can be derived using the dispersion relation from observed swell properties. The solution of the dispersion relation with respect to water depth d :

$$d(L_p, \omega_p) = \frac{L_p}{2\pi} \operatorname{atanh} \left(\frac{\omega_p^2 L_p}{2\pi g} \right) \quad (5)$$

where g is the acceleration of gravity, ω_p is the angular wave peak frequency ($\omega_p=2\pi/T_p$, T_p is the peak period). The method was approved for different areas and sea states [7] [11]) i.e. for the Duck Research Pier (North-Caroline, USA), Port Phillip (Melbourne, Australia), and around Helgoland Island (German Bight, North Sea).

To complete the bathymetric maps, optical data of the QuickBird satellite are used to map extreme shallow waters, e.g., in near coast areas ($d<210\text{m}$) in order to retrieve the complete topography. The investigations are carried out near Rottenest Island, Australia, where SAR, optical and echo-sounding *in-situ* measurement data are available. The area investigated is indicated by a sliced shore line, complicated underwater topography which includes numerous underwater reefs.

Fig.6 shows the Rottenest Island TS-X Spotlight scene with 40 wave rays. SAR-derived bathymetry (rectangular mesh of 150m horizontal resolution) is shown in Fig.7a (3-D). Data combined with depth derived from optical sensors (QuickBird) by sunlight reflection analysis is shown in Fig.7c. The schema of data fusion is shown in Fig.7b.

The implications of remote sensing data for bathymetry estimation from SAR and optical data are based on different physical backgrounds and mathematical applications, but the results complement each other. The optical data provide depths in shallow water from 0m to about 20m depending on underwater reflection during calm weather condition. The depths estimation from SAR covers the areas between about 100m and 10m water depths depending on sea state and acquisition quality. The depths from about 20m to 10m are the domain where synergy of data from both sources can be applied.

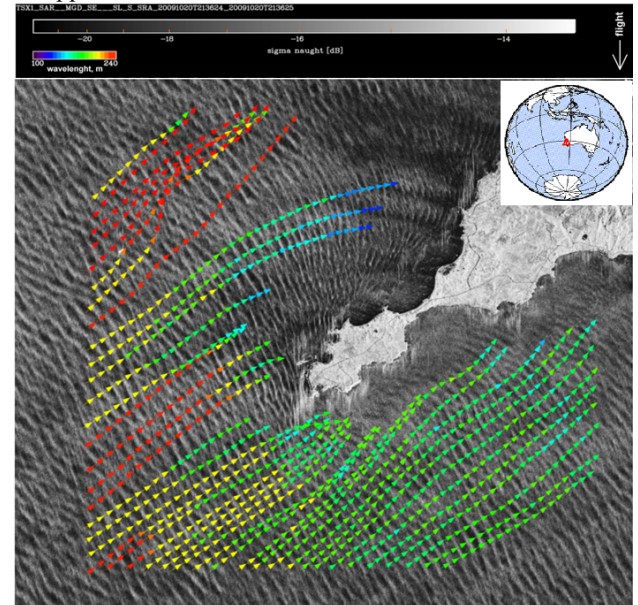


Figure 6. TerraSAR-X Spotlight 10km by 10km coverage acquired on October 20, 2009 over Rottenest Island Australia over Rottenest Island, Australia. 40 wave rays overlap the area are shown.

Fig.8a presents the scheme for comparison of retrieved data with sonar measurements: The TS-X scene is underlying, a white line marks the area for which a comparison is done. The sonar measurement data from different echo-sounding campaigns (measurement errors are unknown) are also integrated and interpolated on rectangular uniform grid $dx=dy=150m$, relative error between both data sets is shown in Fig.8b: assuming the interpolated sonar depths present the real values, then about 50% of the compared area has an error range of about $\pm 10\%$ (shown in white color).

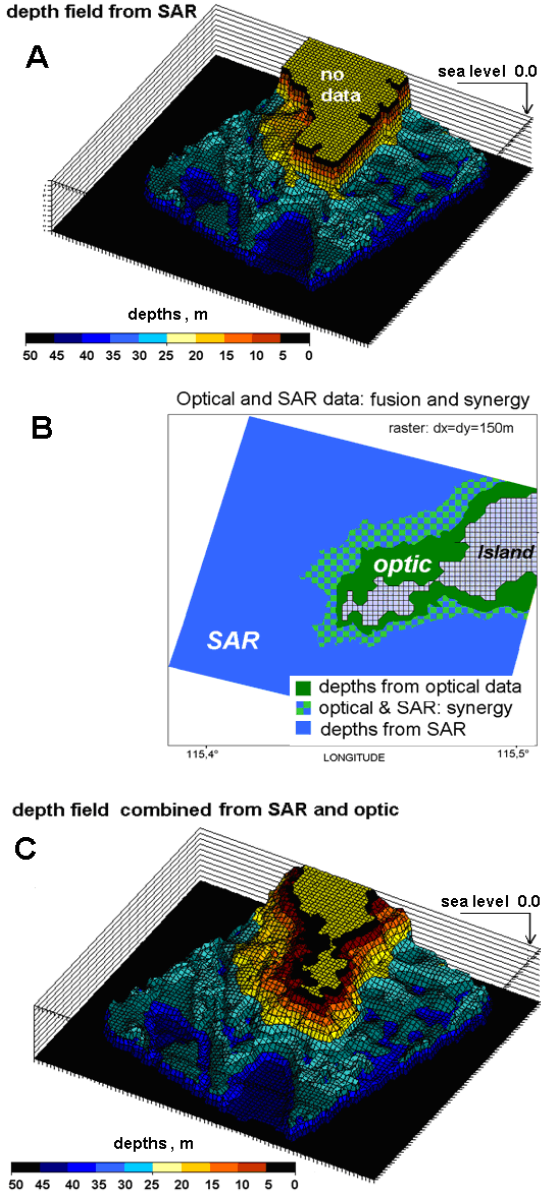


Figure 7. Bathymetry derived from TerraSAR-X (A), scheme of data fusion and synergy of optical and SAR data (B). Depth field obtained from TS-X SAR and optical QuickBird data after fusion and synergy were applied on uniform raster with horizontal resolution of 150m by 150m. The resulting bathymetry field covers the area about 8km \times 8km.

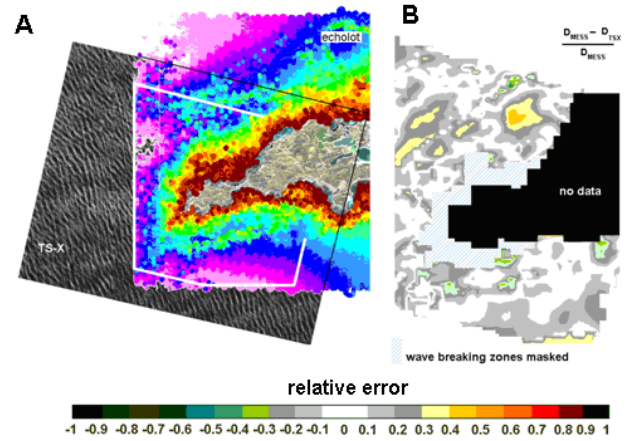


Figure 8. schema for comparison of a sonar measurement to TS-X derived depths (white line marks the comparison area) (A) and relative error for white marked area (wave breaking zones are masked additionally) (B).

There are also more variations (one is located in the north of the Island, between a bank and the coast - the swell waves are slowed down and dissipated over a reef and do not build up anymore in a “bag” between two reef-banks. The wave breakings zones, in front of the coast (depicted by streaks structures) destroy the processing of sub-images and do not allow obtain the wave length accurately. They are masked and taken out from depth estimation processing.

III. IMPLEMENTATION OF SAR RETRIEVED INFORMATION INTO SPECTRAL NUMERICAL WAVE MODELING

Remote sensing data can be used as input and for validation of numerical models. Combining fine resolution remote sensing information with coastal numerical models can help to validate the spatial distribution of sea state parameters in coastal shore zones, where small-scale effects and strong bottom gradients play a role.

A. SAR retrieved information and numerical wave modeling: wind.

The wind information, retrieved from TS-X images are used as input data for the numerical wave K-model [19]. The K-model is a discrete spectral numerical model developed at GKSS-Research Centre (HZG) and adapted to shallow waters and strong bottom gradients. Being an offspring of the WAM-Model, it contains some different source terms. The wave energy density is simulated by K-model in the wave number k and directional θ_a domain. For more details see [19].

The K-model was applied with a directional resolution $\Delta\theta_a=30^\circ$ for simulation of energy density spectra $E_w(location, k, \theta_a)$ and the wave number is resolved with 25 nodes (frequency space 0-1Hz). The model was implemented on a grid with 100m horizontal resolution for Hörnum Bight area by Sylt Island. The wave energy spectra simulated with temporal resolution of $\Delta t=5sec$ are integrated each 10min to provide the wave parameters wave height H_s ,

periods (T_{m-1} , T_{m-2} , mean and peak periods, etc.) and wave direction. The Stripmap TS-X scene acquired over Sylt Island and Hörnum Bight in German Bight (Fig.3) was used to provide the model input data.

The Hörnum Bight is a closed area where the boundary conditions (wave spectra) only for waves going to north-east play a role. The local wind sea develops quickly and reflects the wind speed and fetch [10]. The wind field U_{10} obtained using TS-X data (XMOD) was applied for Hörnum Bight, the model was run for this wind speed and direction as first ($10\text{m}\cdot\text{s}^{-1}$ at the position where GKSS-Research Center wave rider buoy Hörnum-Tief-1 at $54^{\circ}46'2''\text{N}$ $8^{\circ}22'8''\text{E}$ is located). The comparison with collocated wave rider buoy measurements shows a good agreement with model results: the measured significant wave height is 50cm and the wave model gives $H_s=52\text{cm}$.

A sensitivity study for wave simulation was carried out by changing wind speed and direction. The results (Fig.9) show sensitivity of waves on local wind variation and importance of local wind effects on wave behavior in coastal areas. The varying TS-X retrieved wind speed (increased and decreased at $3\text{m}\cdot\text{s}^{-1}$) results in strong deviation of about $\sim \pm 25\%$ of modeled wave height at buoy position.

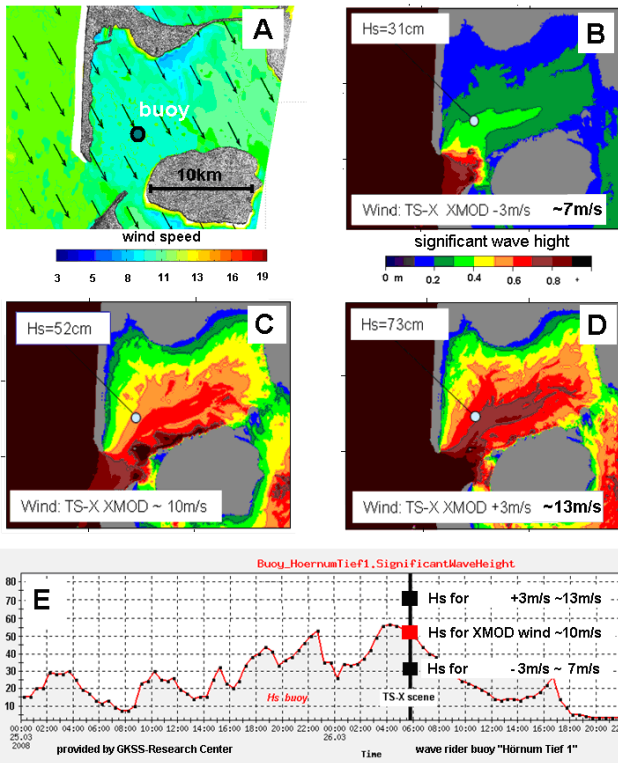


Figure 9. Retrieved wind field (section II.C and Fig.3) shows local variations (A), wave height simulated using TS-X derived wind $\sim 10\text{m}\cdot\text{s}^{-1}$ at buoy position $54^{\circ}46'2''\text{N}$ $8^{\circ}22'8''\text{E}$ (C) corresponds with buoy measurement well (E). Varying the TS-X retrieved wind speed (increased and decreased at $3\text{m}\cdot\text{s}^{-1}$) results strong deviation about $\sim 25\%$ of modeled wave height (B, D).

The changing of the sea state properties influence strongly the results of coupled modeling: the turbulent mixing in the water column and processes at boundary layer water-seabed undergo a significant change in the Wadden shallow-water areas. According to linear wave theory (e.g. [21]) used for technical applications, the wave orbital velocity at the sea bed u_w influences the seabed shear stress velocity u^* , which is responsible for erosion processes [20]. E.g. for $u^* < 0.99\text{ cm}\cdot\text{s}^{-1}$ occurs sedimentation, $1.0 < u^* < 2.8\text{ cm}\cdot\text{s}^{-1}$ means resuspension (of suspended matter that before sunk). The erosion occurs by $u^* > 2.8\text{ cm}\cdot\text{s}^{-1}$. This concept is broadly used by modeling (e.g. [9]) and is a core of the Suspended Matter Transport Model SPMT developed by GKSS Research Center and implemented in the operational system of BSH (German Federal Maritime and Hydrographic Agency) [9].

The value of $u^* = (\tau_w / \rho_w)^{0.5}$, where τ_w is the shear stress at seabed by waves and ρ_w is the water density, will be changed for three different sea states, simulated above (see Table 1, wave periods $T_{m2}=3.2\text{s}$; 3.4s ; 3.6s correspondingly) for the buoy location. The original TS-X wind derived $U=10\text{m}\cdot\text{s}^{-1}$ results in sea state which corresponds to the sedimentation, the wind input increasing at $3\text{m}\cdot\text{s}^{-1}$ switches the system into resuspension, wind input increasing more than $3\text{m}\cdot\text{s}^{-1}$ will result in a switching to erosion.

These variations show sensitivity of the coupled model systems to wind input in respect not only to waves but also to wave dependent parameters and processes like suspended matter transport, morphodynamics and sand transport.

TABLE 1.
MORPHODYNAMIAL PROCESSES DEPENDENT ON SEA STATE PARAMETER FOR THE BUOY LOCATION

Wind, $\text{m}\cdot\text{s}^{-1}$	H_s , cm	u_w , $\text{cm}\cdot\text{s}^{-1}$	u^* , $\text{cm}\cdot\text{s}^{-1}$	morphodynamics process
7	31	1.2	0.3	sedimentation
10	52	3.6	0.7	sedimentation
13	73	7.8	1.3	resuspension

B. SAR retrieved information and numerical wave modeling: wind and boundary conditions.

TS-X Spotlight scene acquired in the North Sea on Feb. 25, 2009 over Helgoland Island (see Fig.5) provides the swell waves with about 0.3-1m wave height propagating in the direction SE into the German Bight. The wind field was retrieved going-to North-East with mean speed about $13\text{m}\cdot\text{s}^{-1}$. This corresponds well to DWD wind forecast, wind field U_{10} obtained using XMOD. The information derived from TS-X image was used to provide an input into the wave model.

For the Helgoland area the K-model was implemented on a grid with 100m horizontal resolution (Fig.10, right). For this area (open North Sea) wind forcing and boundary wave spectra are necessary for numerical simulations. For the boundary the spectra including the swell (obtained using XWAVE algorithm) and wind-sea (JONSWAP spectra using TS-X wind derived) were applied. The wave height (swell) at the boundary is about 1m, which agrees well to

results from the WAM model for the German Bight (forecast by www.dmi.dk). The model results are stored separately and gathered for wind-sea and swell parts of the waves (the k-spaced energy spectra are converted to frequency domain). The shoaling, refraction and shadowing effects of the islands on the wave height are well visible in Fig.10.

SUMMARY

New X-band retrieval schemes were developed to estimate wind and ocean wave parameters. The SAR data can be applied to validate spectral numerical wave models. Investigation of calibrated SAR Spotlight images from the TerraSAR-X Satellite shows that it is possible to detect individual waves up to 30m wavelength, their refraction and wave shoaling due to high spatial resolution of images. The underwater structures e.g. banks, bars and reefs can be detected by long wave refraction. The wave energy flux, important for coastal equipment protection can be estimated using SAR information and by applying wave ray tracking techniques.

A new way to explore and obtain underwater topography by remote sensing data and using synergy of different data sources is presented. The depth can be obtained with accuracy of order +/- 15% for depths 60m-10m using SAR methods depending on image acquisition quality, sea state and the complexity of the topography (e.g. reefs cause wave breaking).

The SAR-based methodology allows also certain detecting shallows (underwater mountains, reefs, deposited sand bars) with depths <30m, even the quality of sea state does not allow obtaining the topography exactly. Such a product can be applied to specify an exact instruction for vessel measurement. This kind of information is important for e.g. German Bight, where the topography changes relatively fast due to soft seabed, so that the official charts can be out of date. The information about shallows detected (reefs) can be applied for ship safety.

ACKNOWLEDGMENTS

This study is supported by projects *DEEPVIEW* (Bathymetry from TerraSAR-X und RapidEye Satellites) and *DeMarine PAROL* Ship Security supported by DLR Space Agency and BMWi.

REFERENCES

- [1] Behrens, A. and H. Günther, "Operational wave prediction of extreme storms in Northern Europe", in: *Natural Hazards*, doi: 10.1007/s11069-008-9298-3, 2008.
- [2] Borge, J.N., Rodriguez, G. Hessner, K. and P.González, "Inversion of marine radar images for surface wave analysis", in *J. Atmos. Oceanic Technolo*, Vol. 21, 2004.

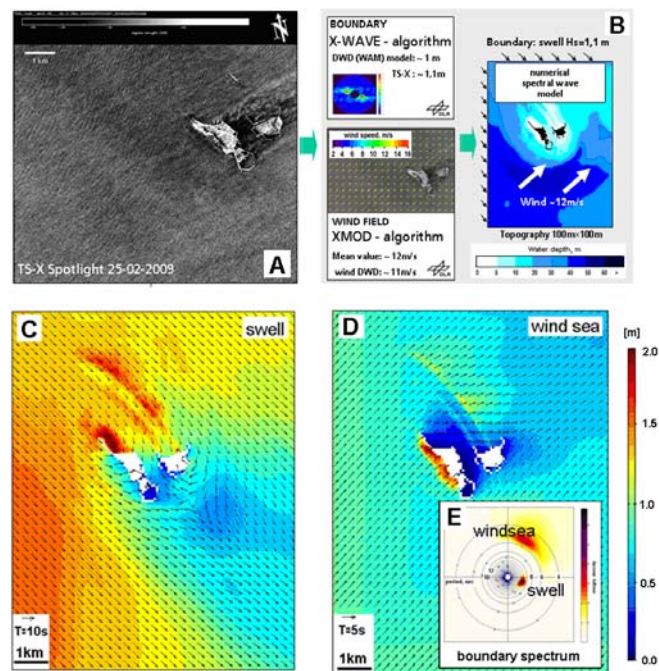


Figure 10. SAR-retrieved information as input data for numerical modeling: wind and boundary conditions. TS-X Spotlight (A). Schema of data implementation (B). The results: significant wave height fields for swell (C) and wind-sea (D). The spectral wave model run for Helgoland Island area, simulated on mesh of 100m horizontal resolution (arrows are plotted in 5 grid point steps, arrows length means value of T_{m-1} period, arrows direction is the wave mean direction). The spectrum obtained from TS-X scene and applied as boundary condition for numerical simulations (E).

- [3] Breit,H., Fritz,T., Balss,U., Lachaise, M., Niedermeier, A. and Martin Vonavka, "TerraSAR-X SAR Processing and Products" in: *IEEE TRANSACTIONS ON GEOSCIENCE AND REMOTE SENSING*, VOL. 48, NO. 2, FEBRUARY 2010. 0196-2892/\$26.00 © 2009 IEEE.
- [4] Bruck, M. and Susanne Lehner, "Extraction of wave field from TerraSAR-X data" in: *Oceanography workshop SEA-SAR 2010, Advances in SAR Oceanography from ENVISAT, ERS and ESA third party missions*, ESA ESRIN, Frascati/Rom, Italy, 25-29 January 2010.
- [5] Bruns, T. 2010. German Weather Service DWD, wave forecasting. Private communication.
- [6] Bruns, T., Li, X-M. and S. Lehner „Global Wave Model Validation Using ENVISAT ASAR Wave Model Data“, this issue.
- [7] Brusch, S., Held, P., Lehner, S., Rosenthal, W., Pleskachevsky, A. "Underwater Bottom-Topography in coastal areas from TerraSAR-X data", in: *International Journal of Remote Sensing*, *in print*.
- [8] Gayer, G., S. Dick, A. Pleskachevsky, and W. Rosenthal, "Numerical modeling of suspended matter transport in the North Sea". *Ocean Dynamics*, **56**, 62-77. 2006.
- [9] Gayer, G., Dick, S., Pleskachevsky, A., Rosenthal, W., "Modelling of suspended particulate matter in North and Baltic seas". BSH-reports, N36, 50 pp. 2004.

- [10] Pleskachevsky, A., Eppel, D., Kapitza, H., "Interaction of Waves, Currents and Tides, and Wave-Energy Impact on the Beach Area of Sylt Island", *Ocean Dynamic* s. Volume 59, Issue 3/ June 2009.
- [11] Pleskachevsky, A., Li, X.-M., Bruschi, S., and Susanne Lehner, "Investigation of wave propagation rays in near shore zones", *Oceanography workshop SEA-SAR 2010, Advances in SAR Oceanography from ENVISAT, ERS and ESA third party missions*, ESA ESRIN, Frascati/Rom, Italy, 25-29 January 2010.
- [12] Lehner, S., Horstmann, J., Koch, W., & Rosenthal, W., "Mesoscale wind measurements using recalibrated ERS SAR images", *JGR-Oceans* 97JC02726 Vol. 103, No. C4, p. 7847, 1998.
- [13] Lehner, S.; Schulz-Stellenfleth, J., Bruschi, S., Li, X. M., "Use of TerraSAR-X Data for Oceanography", *EUSAR 2008, 7th European Conference on Synthetic Aperture Radar*, Friedrichshafen, Germany 06/02/2008 - 06/05/2008.
- [14] Li, X.-M., Lehner, S., Bruschi, S., and Y.-Z. Ren, "Sea surface wind measurement over offshore wind farm using TerraSAR-X data" *Proc. of SPIE 2011 conference - Remote Sensing of the Ocean, Sea Ice, Coastal Waters, and Large Water Regions 2011*.
- [15] Lyzenga, D. R., R. A. Shuchman, and J. D. Lyden, "SAR imaging of waves in water and ice: evidence for velocity bunching", *J. Geophys. Res.*, 90, 1031-1036, 1985.
- [16] Pontes, M., Bruck, M., Lehner, S., and A. Kabuth, "Using Satellite Spectral Wave Data for Wave Energy Resource Characterization", 3rd International Conference on Ocean Energy, 6 October, Bilbao.
- [17] Ren, Y.-Z., Lehner, S., Li, X.-M., He, M.-X., Bruschi, S., "Retrieval Algorithm of Sea Surface Wind Field Using X-band TerraSAR-X Data", *IEEE Transactions on Geoscience and Remote Sensing*, submitted.
- [18] Rosenthal, W., Pleskachevsky, A. L., Lehner, S. and S. Bruschi, "Observation and Modeling of High Individual Ocean Waves and Wave Groups Caused by a Variable Wind Field", *this issue*.
- [19] Schneggenburger, C., H. Günther and W. Rosenthal, "Spectral wave modeling with non-linear dissipation: validation and applications in a coastal tidal environment", in: *Coast Eng* 41, 201-235.
- [20] Solsby, R. "Dynamics of marine sands. A manual for practical application". Thomas Telford Services, London, 1997
- [21] Svendsen, A. and I.G. Jonsson, "Hydrodynamic of coastal regions". ISBN 87-87245-57-4. Stougaard Jensen/Kobenhavn. 1982.
- [22] Winkel, N., "Modeling of waves in extreme shallow water", *GKSS-Research Center*, ISSN 0344-9629, 1994.
- [23] Witte, J-O, Kohlhase S, Radomski J, Fröhle, "Fallstudie Sylt, Teilprojekt Strategien und Optionen der Küstenschutzplanung für die Insel Sylt", Technical report, Institut für Wasserbau der Universität Rostock, Wismar, 2002.